

Improved QRS Detection Algorithm using Dynamic Thresholds

Mohamed Elgendi, Mirjam Jonkman, Friso De Boer
*School of Engineering and Information Technology,
Charles Darwin University, Australia*

Abstract

The accurate detection of QRS complexes is important for ECG signal analysis. This paper presents an improved version of a QRS detector based on an adaptive quantized threshold. The algorithm achieves high detection rates by using automatic thresholds instead of predetermined static thresholds. We improved the number of detected QRS in non-stationary random arrhythmic ECG signals by applying a secondary threshold. The performance of the algorithm was tested on 19 records of the MIT/BIH Arrhythmia Database resulting in 97.5% sensitivity and 99.9% positive predictivity.

1. Introduction

The electrocardiogram (ECG) is a graphical representation of the electrical activity of the heart. ECG signals are obtained by connecting specially designed electrodes to the surface of the body. It has been in use as a non-invasive cardiac diagnostic tool for over a century. For continuously monitoring the electrical activity of the heart for 24 hours or more, the portable Holter monitor is used. A robust automated algorithm that can analyze the 24 hours recordings is needed.

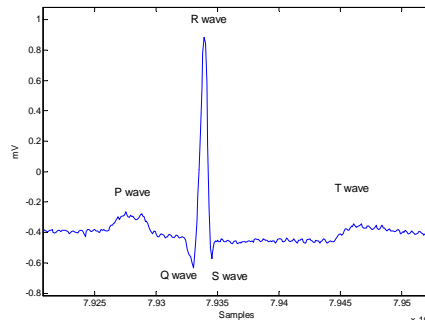


Figure.1. ECG for a single cardiac cycle

Most of the cardiac disease classification algorithms begin with the separation or delineation of the individual ECG signal main waves. The ECG signal of a single cardiac cycle consists of the QRS complex, P and T waves as shown in Figure 1. Occasionally a U-wave may also be present which lies after the T-wave.

The QRS complex is the most noticeable part in the ECG because of its high amplitude compared to the P and T waves. QRS complex represents the depolarization of the ventricles of the heart which have greater muscle mass and therefore its process consumes more electrical activity.

The automatic detection of QRS is critical for reliable Heart Rate Variability (HRV) analysis, which is recognized as an effective tool for diagnosing cardiac arrhythmias [1-5], understanding the autonomic regulation of the cardiovascular system during sleep and hypertension [6,7], detecting breath disorder like Obstructive Sleep Apnea Syndrome [8,9], and monitoring other structural or functional cardiac disorders.

The detection of QRS complexes has been extensively investigated in the last two decades. Many attempts have been made to find a satisfying universal solution for QRS complex detection. The difficulties arise mainly because of the huge diversity of the QRS complex waveforms, abnormalities, low signal-to-noise ratio (SNR) and the artefacts accompanying the ECG signals. The motivation behind this work is to increase the accuracy of QRS detection in Arrhythmia ECG signals that suffer from non-stationary random effects, low signal-to-noise ratio (SNR), negative QRS, and low-amplitude QRS.

In 1992, Xue *et al.* [10] developed an adaptive matched filtering algorithm based upon an artificial neural network. Xue *et al.* reported Sensitivities (Se) of 99.84% and 99.09 % and Positive Predictivities (+P) of 99.61% and 98.59 % based on just two records, 105 and 108 from the MIT-BIH Arrhythmia Database [11]

In 1995, Li *et al.* [12] have used wavelet transforms for detection. They reported 0.15 % false detections based on 46 files from the MIT-BIH Arrhythmia Database [11], excluding files 214 and 215.

In 2002, Moraes *et al.* [13] logically combined two different algorithms working in parallel the first adopted from the work of Englese and Zeelenberg [14], the second based on Pan and Tompkins [15] and Ligtenberg and Kunt [16]. Moraes *et al.* reported Sensitivity (Se) = 99.22 % and Specificity (Sp) = 99.73 % after having excluded records of patients with pacemakers. However, they also excluded recordings 108, 200, 201 and 203, from the MIT-BIH Arrhythmia Database [11].

In 2005, Alvarado *et al.* [17] have used the Continuous Spline Wavelet Transform using local maxima of the Continuous Wavelet Transform at different scale. They reported Se = 99.87 % and Positive Predictivity = 99.82 % after using just 9 files out of 48 files from MIT-BIH Arrhythmia database [11].

In 2007, Zhang *et al.* [18] have used the Continuous Wavelet Transform using fixed thresholds. They reported accuracy = 99.5 % after using just 8 files out of 48 files from MIT-BIH Arrhythmia database [11].

In 2008, Chouhan *et al.* [19] have used the first derivative with adaptive quantized thresholds. They reported Se = 98.56 % and Sp = 99.18 % after using 125 files from the CSE Database [20]. They did not apply their algorithm to the MIT-BIH Arrhythmia database [11].

The advantage of using first derivative based methods is that they are less complex to implement than other methods. Here we propose an improved algorithm applying dynamic thresholds. We evaluated the robustness of the method proposed by Chouhan *et al.* [19] and our improved algorithm, applying both algorithms to ECG signals that suffer from, arrhythmia, non-stationary random signals, low signal-to-noise ratio (SNR), negative QRS, low-amplitude QRS and wide premature ventricular beats.

2. Methodology

The electrical activity of the heart originates in the sinoatrial node (SA node), situated in the wall of the right atrium. The impulse then rapidly spreads through the right atrium to the atrioventricular node (AV node). After a delay at AV node, the impulse travels slowly through the bundle of his, the bundle branches, the Purkinje network, and finally the ventricular muscle [21]. The conduction disturbances of this wave can be delayed or block at any point. Three main types of QRS waves, positive (+ve) polarity R-peak, negative (-ve) polarity R-peak, and low polarity as shown in Fig.2

The R-peak with positive polarity, shown in Figure.2(a), is the standard representation of ECG beats. As shown in Figure.2(b), R-peaks with negative polarity can occur because some extrasystoles (especially the ventricular extrasystole) lead to a sudden polarity change. Figure.2(c) shows R-peaks with low amplitude

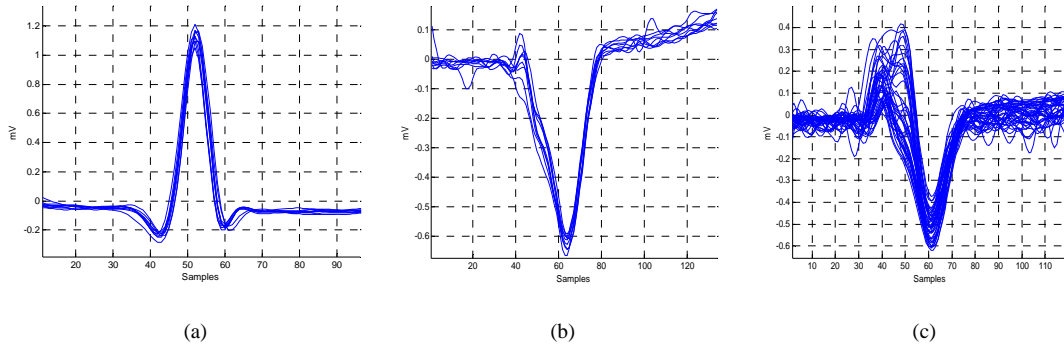


Figure.2. QRSs of three types of R-peak (a) +ve R (b) -ve R (c) low amplitude R

Pang, *et al.* [22] excluded the beats with negative polarity in the detection of heart ischemia. If the polarity of the new beat suddenly changes, then its parameters will not be extracted. Therefore, an algorithm that detects R peaks with positive and negative polarities is required.

The main difficulties in QRS complex detection can be summarized as follows: 1) negative QRS polarities (as discussed above), 2) low SNR (noisy ECG signal), 3) non-stationarity (statistical properties of the ECG signals change with time), 4) low QRS amplitudes, and 5) ventricular ectopics.

Two methods are evaluated in this paper:

- 1) Method I is the method used by Chouhan *et al.* [16] who tested the algorithm on the CSE database [17] only. Here we evaluate the robustness of this method by applying it to the MIT-BIH database [10].
- 2) Method II is the improved method, proposed by the authors. It is tested using the MIT-BIH database [10] and compared with Method I.

The performance of the two methods is evaluated by comparing the detection rates with respect to the number of beats tested.

2.1. Method I: First Derivative of the ECG Signal with Adaptive Quantized Threshold

The method (Method I) used by Chouhan *et al.* [19] (as shown in Figure.4) uses the first derivative with adaptive quantized thresholds. It was previously tested on the CSE database [20], which contains 125 cases of 12-lead simultaneously recorded ECG of 10 seconds duration each, sampled at a rate of 500 Hz. Thus each of the 1500 (125x12) records has 5000 sampling instants.

Here, our motivation is to evaluate the robustness of Method I by applying it to the MIT-BIH Arrhythmia database [11]. The MIT-BIH Arrhythmia database contains records of 30 min duration each, sampled at 360 Hz. We selected records that contain premature atrial beats, premature ventricular beats, and ventricular ectopic beats with low SNR, inverted QRS polarity, and low-amplitude QRS; in total 19 records. Each record contains two leads. We use Lead I from each record in blocks of 3600 samples.

The main steps of Method I are briefly described below:

1. Remove baseline wander as described by Chouhan *et al* [23] as shown in Figure.3.

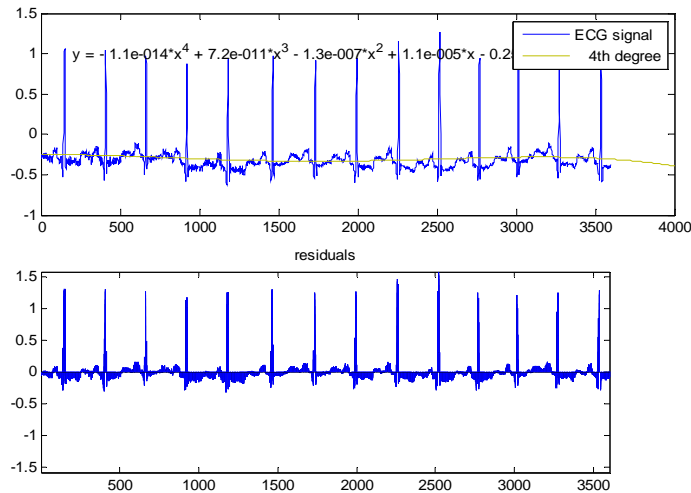


Figure.3. A 4th order polynomial baseline wander removal

2. Extract QRS-feature signal F_Q defined for each of the 3600 sample values of the ECG signal and normalize it by dividing it by the maximum value.
3. Find those portions of F_Q with QRS-candidate marking pulses C_Q , which exceed 5% of the normalized peak magnitude of F_Q .
4. Define a range of normalized adaptive amplitude thresholds [19] and by taking one threshold at a time,
5. Test whether the peak value of F_Q crosses the threshold

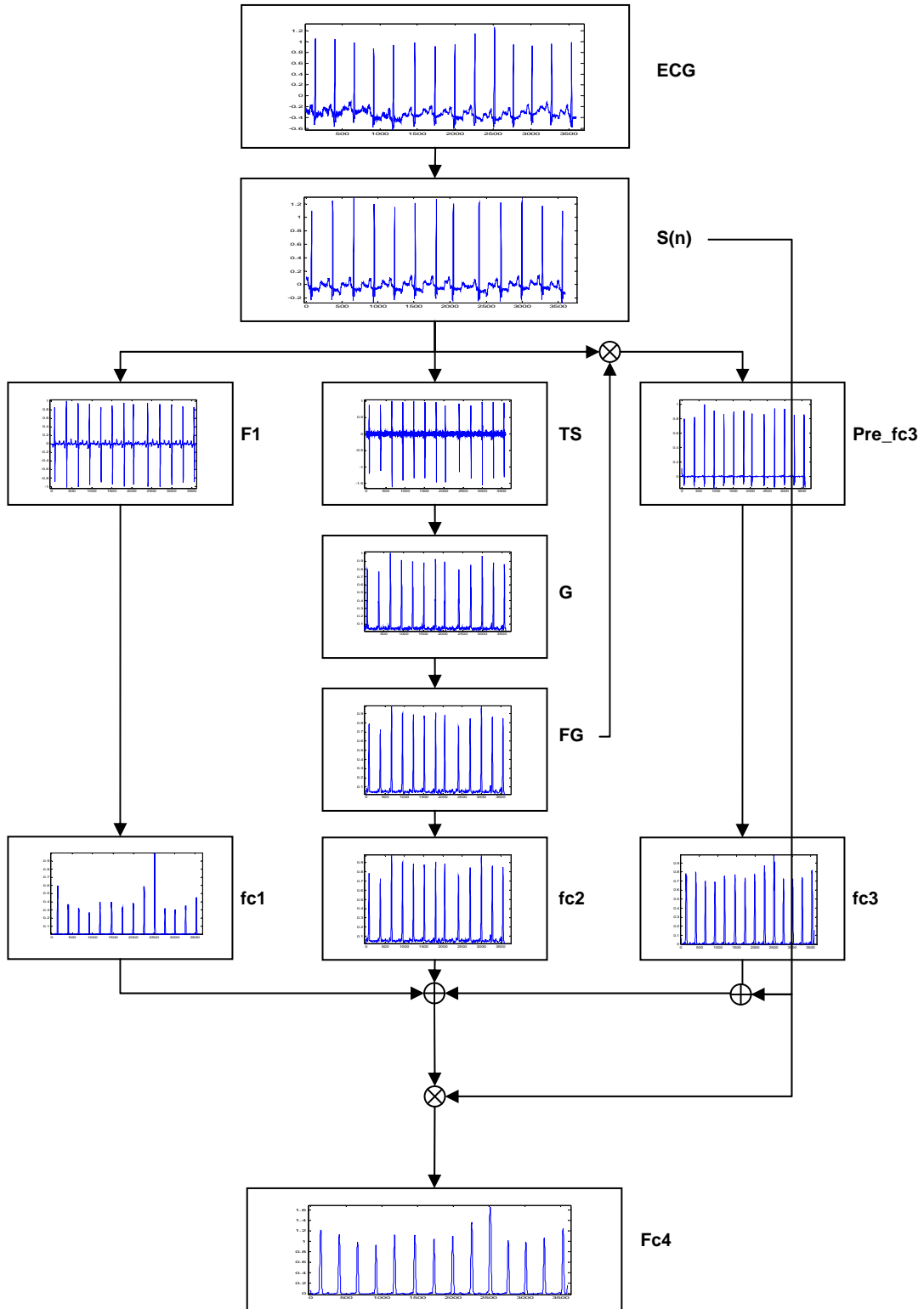


Figure.4. Flow Chart of Method 1

6. Demarcate detected QRS-complexes D_Q for lead I of a given case, count and list the number of D_Q , that is, number of QRS-detections and compute statistical properties for these numbers of detections for the case [19].

When using multiple leads, select all the QRS-detections, demarcated by QRS-detection marking pulses D_Q with:

- (a) minimum value of standard deviation
- (b) the corresponding value of median equal to the correct and reliable number of QRS-complexes in that case, evaluated by algorithm [12]
- (c) Demarcate the first column out of these QRS detections [19] with QRS Marking Pulses MP_Q . That is, the first out of multiple correct QRS detections demarcated by D_Q are declared as the *final QRS-detection* and the corresponding marking pulses are designated as MP_Q .

These final QRS marking pulses MP_Q delineate the QRS-complexes in the given ECG signal. The portions of the ECG signal within these marking pulses MP_Q are the detected QRS complexes with the presented algorithm.

2.2. Method II: Improved method using a Dynamic Threshold

Method II has a slightly different structure from Method I (as shown in Table.1 and Figure. 5)

TABLE I
 MAIN DIFFERENCES BETWEEN METHOD 1 AND METHOD 2

Method 1	Method2
• S is 4 th order polynomial baseline removal	• S is Butterworth filter (1-13Hz)
• F1 is the first derivative of S	• F1 is the square of S
• TS is sigmoid function of S	• TS is sigmoid function of S
• fc1 is zero-crossing threshold applied to F1	• FG1 is moving average filter of G1 which is the gradient of F1
• fc2 is zero-crossing threshold applied to FG which is moving average filer of G (the gradient of TS)	• FG2 is moving average filter of G2 which is the gradient of TS
• fc3 is zero-crossing threshold derived from Pre-fc3 which is the product of S and FG	• FG3 is moving average filter of G3 which is the gradient of Pre-fc3 (the product of S and FG2)
• Pre-fc4 = [fc1+fc2+fc3+abs(S)]*abs(S)	• Pre-fc4 = FG1+FG2
• fc4 is zero-crossing threshold applied Pre-fc4	• FG4 is moving average filter of Pre-fc4
	• fc4 is threshold consists of THR1 and THR2 applied to Pre-fc4

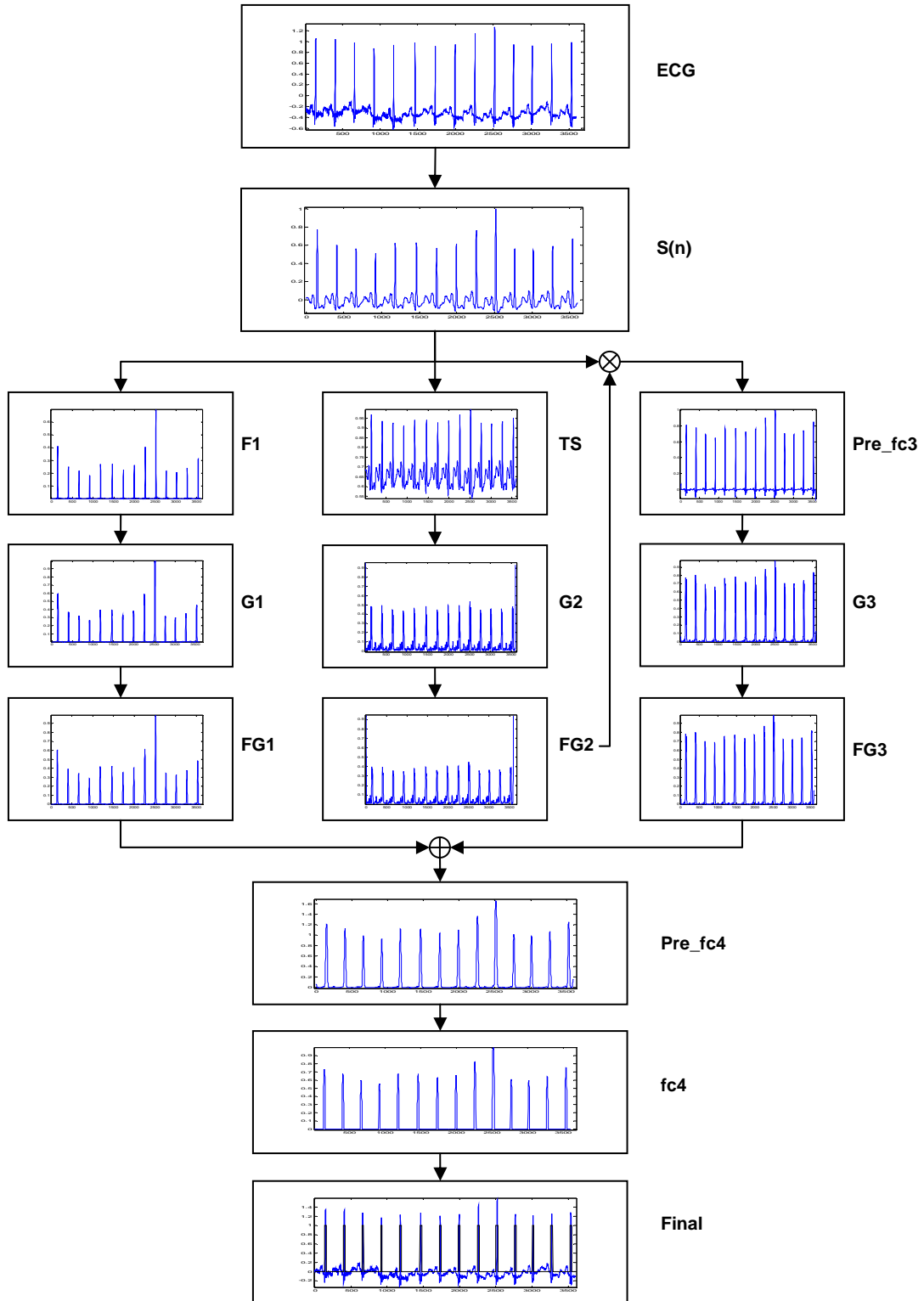


Figure.5. Flow Chart of Method 2

The main procedural difference steps between Method II and Method I (as shown in Table.1.) are the following:

1. Remove the baseline wander and undesired frequencies: In order to remove all frequencies which are not necessary to detect the region of the QRS complex, we applied a Butterworth filter with passband of 1-13Hz (as shown in Figure.6. and Figure.7) rather than fourth polynomial filter used to remove the baseline wander by Chouhan *et al.* [23] (as shown in Figure.3) which removes some frequencies contributing to the detection of QRS complex region.

$$S(n) = \text{Butterworth}(\text{ECG}(n), 1 - 13\text{Hz})$$

The filtering removes not just baseline wander and high frequency noise but also frequencies of the actual ECG signal. However these frequencies do not contribute to detect the QRS complex and detection is improved by removing these frequencies.

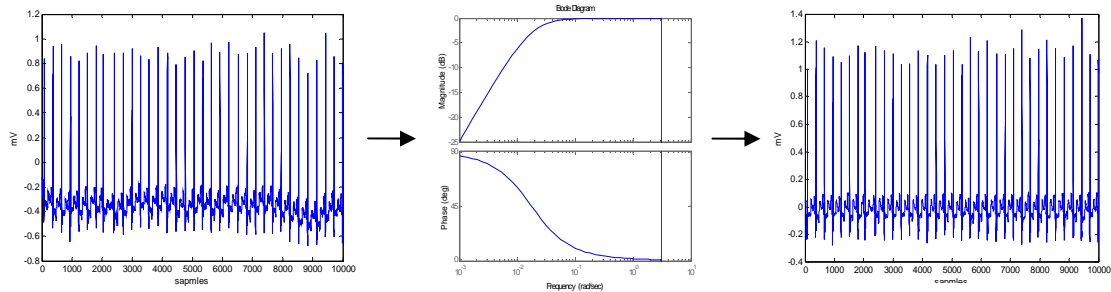


Figure.6. low pass filter

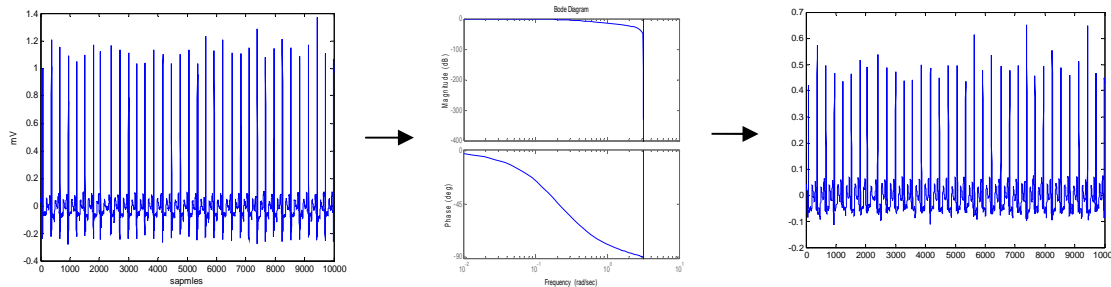


Figure.7. high pass filter

2. The mean is subtracted from the signal block.

$$S(n) = S(n) - \text{mean}(S(n))$$

3. $F1(n)$ is the square of the filtered ECG signal ($S(n)$) makes the results positive and emphasizes large differences resulting from QRS complexes rather than using the first derivative as Chouhan *et al.* [19].

$$F1(n) = [S(n)]^2$$

4. FG1, FG2, FG3, and FG4 are moving average filters with rectangular sliding of 21 sample points from (n-10) to (n+10) with center at (n).

$$\begin{aligned} FG1(n) &= \frac{1}{21} \sum_{i=n-10}^{n+10} G1(i), & FG2(n) &= \frac{1}{21} \sum_{i=n-10}^{n+10} G2(i), & FG3(n) &= \frac{1}{21} \sum_{i=n-10}^{n+10} G3(i), \\ FG4(n) &= \frac{1}{21} \sum_{i=n-10}^{n+10} pre_fc4(i) \\ n &= 1, 2, \dots, 3600 \end{aligned} \quad (1)$$

The window size depends on the sampling frequency of the collected ECG data. For sampling frequency of 360Hz, a window size of 21 points corresponds to approximately half of the QRS duration.

5. Pre_fc3 is the product of FG2 with filtered ECG signal S(n) to enhance the slope of QRS. In Chouhan *et al.* [19], FG2 is called FG.
6. fc3 is the sum of FG1 with FG2. In Chouhan *et al.* fc3 calculated from Pre_fc3 directly.
7. The desired final QRS feature signal FQ is derived by retaining the amplitude values of G4 exceeding Dynamic Threshold THR1 rather than a static threshold of 5% of the maximum peak amplitude and reducing the remaining to zero. THR1 equals the mean of G4 + Standard deviation of G4.

$$\begin{aligned} fc4(n) &= \begin{cases} G4(n), & FG4(n) > THR1 \\ 0, & \text{otherwise} \end{cases} \\ THR1 &= \text{mean}(fc4) + \text{std}(fc4) \\ n &= 1, 2, \dots, 3600 \end{aligned} \quad (3)$$

8. 'F_Q' is demarcated by QRS candidate marking pulses C_Q of unit amplitude, marking the QRS candidate region, using the relation:

$$\begin{aligned} C_Q(n) &= \begin{cases} 1, & F_Q(n) > 0.01 \\ 0, & \text{otherwise} \end{cases} \\ n &= 1, 2, \dots, 3600 \end{aligned} \quad (4)$$

9. The number of QRS candidates is counted by finding the indexes of Onset/Offset for each QRS as following:

$$\begin{aligned} \text{OnsetOffset_indexes} &= \text{find}(\text{abs}(\text{diff}(C_Q(n))) > 0) \\ n &= 1, 2, \dots, 3600 \end{aligned} \quad (5)$$

where, $\text{abs}(\text{diff}(C_Q))$ is the absolute value of the difference of C_Q.

The amplitude of the R peaks from each consecutive onset index and offset index from F_Q are stored in an array. The number of the values in this array is the number of QRS peaks detected.

10. QRS complexes around wide premature ventricular beats and ventricular ectopic beats are detected. If the following condition is satisfied we replace previously detected QRS complexes with zeros.

$$\frac{\text{length}(\text{find}(\text{fc4}) > \text{THR2})}{3600} > 0.05 \quad (6)$$
$$\text{THR2} = 2 * \text{std}(\text{fc4})$$

Steps 1 to 9 are then repeated to detect QRS complexes that were previously missed.

11. The RR intervals are stored in an RR array.

12. Detect QRS complexes with low amplitudes: After step (a), we detect the low amplitude QRS between each RR interval greater than threshold (THR3),

$$\text{THR3} = 1.5 * \text{mode}(\text{RR}) \quad (7)$$

where, mode(RR) is the most frequent RR interval. THR3 depends on the local heart rate of that signal block rather than a static threshold.

3. Results

The QRS detection algorithms were evaluated using the following statistical parameters:

$$Se = \frac{TP}{TP + FN} \quad (8)$$
$$+P = \frac{TP}{TP + FP}$$

where TP is the number of true positives (QRS complexes detected as QRS complexes), FN is the number of false negatives (NOT QRS complexes detected as QRS complexes), and FP is the number of false positives (QRS complexes detected as NOT QRS complexes).

The sensitivity Se reports the percentage of true beats that were correctly detected by the algorithm. The positive predictivity $+P$ reports the percentage of beat detections which were in reality true beats.

Method I and Method II were both applied to the MIT-BIH Arrhythmia database. As shown in Table 2, Method I scored $Se=87.9\%$ and $+P=97.6\%$ over 44677 beats. However, Method I achieved poor sensitivity rates for records 200, 215, 228 and 233 which suffer from negative QRS polarities and ventricular ectopics, resulting in a high number of false negatives (FN). Method I also has a very poor positive predictivity for record 117 which has a low SNR and low amplitude R peaks.

TABLE II
 METHOD I PERFORMANCE ON MIT-BIH DATABASE

Record	No of beats	TP	FP	FN	SE	+P
100	2258	2197	7	42	98.1%	99.7%
101	1860	1769	0	39	97.8%	100.0%
103	2078	2023	0	41	98.0%	100.0%
108	1900	1497	14	88	94.4%	99.1%
112	2528	2051	0	28	98.7%	100.0%
116	2404	2051	5	59	97.2%	99.8%
117	1530	1507	909	7	99.5%	62.4%
121	1856	1796	7	27	98.5%	99.6%
200	2593	853	9	1604	34.7%	99.0%
202	2128	2058	22	50	97.6%	98.9%
205	2648	2275	3	293	88.6%	99.9%
209	2997	2906	9	33	98.9%	99.7%
213	3241	2699	34	90	96.8%	98.8%
215	3353	1639	2	837	66.2%	99.9%
220	2041	2006	0	17	99.2%	100.0%
223	2581	2256	2	48	97.9%	99.9%
228	2047	688	10	1289	34.8%	98.6%
231	1565	1539	0	18	98.8%	100.0%
233	3069	632	1	226	73.7%	99.8%
Total	44677	34442	1034	4836	87.9%	97.6%

The improved algorithm is more efficient in detecting QRS complexes around ventricular ectopics. Figure.8 shows correct detection of QRS complexes around three ventricular ectopics with same morphology. As shown in Figure.9, the algorithm can also detect QRS complexes around ventricular ectopics with different morphologies.

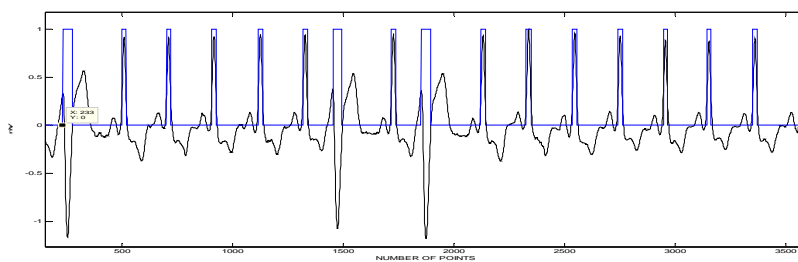


Figure.8. Detected QRSs around three uniform ventricular ectopics (same morphology)

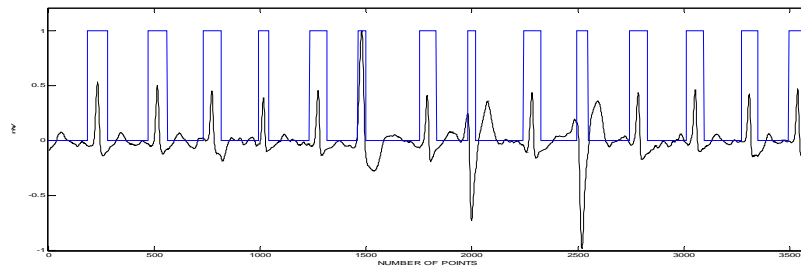


Figure.9. Detected QRSs around three multiform ventricular ectopics (different morphology)

TABLE III
 METHOD II PERFORMANCE ON MIT-BIH DATABASE

Record	No of beats	TP	FP	FN	SE	+P
100	2258	2257	0	12	99.5%	100.0%
101	1860	1853	3	10	99.5%	99.8%
103	2078	2067	0	13	99.4%	100.0%
108	1900	1731	5	30	98.3%	99.7%
112	2528	2514	0	14	99.4%	100.0%
116	2404	2376	4	19	99.2%	99.8%
117	1530	1521	2	14	99.1%	99.9%
121	1856	1844	1	18	99.0%	99.9%
200	2593	2248	0	222	91.0%	100.0%
202	2128	2088	9	16	99.2%	99.6%
205	2648	2613	1	41	98.5%	100.0%
209	2997	2957	2	32	98.9%	99.9%
213	3241	3199	0	36	98.9%	100.0%
215	3353	3307	3	58	98.3%	99.9%
220	2041	2033	0	11	99.5%	100.0%
223	2581	2532	0	39	98.5%	100.0%
228	2047	1966	3	127	93.9%	99.8%
231	1565	1561	4	21	98.7%	99.7%
233	3069	2676	0	491	84.5%	100.0%
Total	44677	43343	37	1224	97.5%	99.9%

The improved algorithm (Method II) also detects more low amplitude R-peaks correctly, as can be seen from Fig 10.

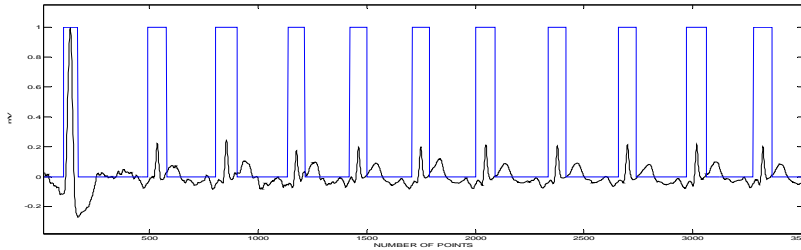


Figure.10. Detect QRSs with low amplitudes and one ventricular ectopic

In addition Method II successfully detects QRS complexes with low SNR and QRS complexes with negative polarities; see Figure.11 and Fig 12.

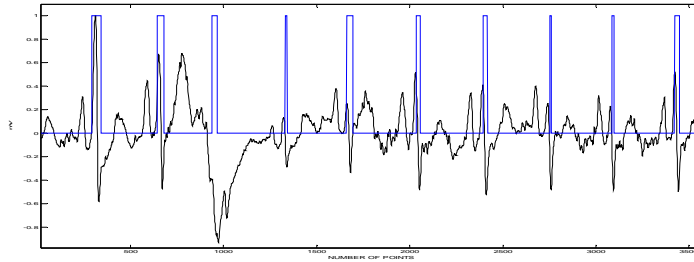


Figure.11. Detect QRSs with low SNR

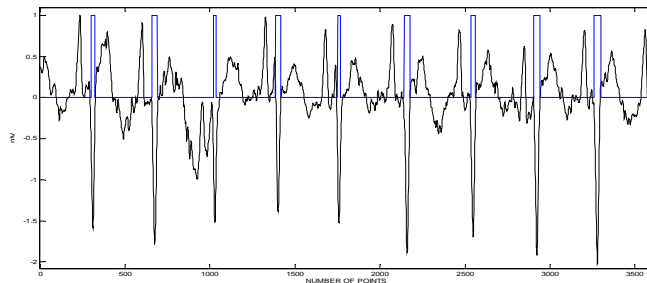


Figure.12. Detect negative QRSs with low SNR

As a result of the improved detection of QRS complexes in records which suffer from negative QRS polarities and ventricular ectopics Method II achieves significantly improved sensitivity rates compared to Method I (see Table 2 and 3) in particular for records 200, 215, 228 and 233. In addition Method II achieves improved positive predictivity in particular for record 117 which has a low SNR and low amplitude R peaks (see Table 2 and 3). Overall, Method II scored $Se=97.5\%$ and $+P=99.9\%$ over 44677 beats.

Table IV compares the performance of Method I applied to the CSE database, as reported by Chouhan *et al.* [16], Method I and Method II both applied to MIT-BIH Arrhythmia database [10].

TABLE IV
 PERFORMANCE OF QRS DETECTION ALGORITHMS APPLIED
 ON DIFFERENT DATABASES

Methodology	Database used	No of beats	SE	+P
Method I	CSE-dataset3	17729	98.56%	99.18%
Method I	MIT-BIH Arrhythmia	44677	87.9%	97.6%
Method II	MIT-BIH Arrhythmia	44677	97.5%	99.9%

4. Conclusion

QRS detection methods are affected by the quality of the ECG recordings and the abnormalities in the ECG signals. The proposed algorithm introduces a secondary dynamic threshold to improve the accuracy of detection of QRS complexes in records with low signal-to-noise ratio, negative QRS polarities, low-amplitude R peaks, and ventricular ectopics.

We compared the improved algorithm to the method described by Chouhan et al. [19] by applying both algorithms against 19 records of the standard MIT-BIH database. It was shown that the new algorithm achieves significantly better detection rates compared to the method of Chouhan et al. with overall 97.5% sensitivity and 99.9% positive predictivity.

5. References

- [1] Thong, T., J. McNames, M. Aboy, B. Goldstein, "Prediction of paroxysmal atrial fibrillation by analysis of atrial premature complexes", *IEEE Trans. On Biomed. Eng.*, 51(4), pp. 561-569, 2004.
- [2] Bashour, C.A., M. Visinescu, B. Gopakumaran, O. Wazni, F. Carangio, J.P. Yared, N. Starr, "Characterization of premature atrial contraction activity prior to the onset of postoperative atrial fibrillation in cardiac surgery patients", *CHEST*, 126(4), pp. 831S, 2004.
- [3] Tsipouras, M.G., D.I. Fotiadis, D. Sideris, "Arrhythmia classification using the RR interval duration signal", *Comp. In Card.*, 29, pp. 485-488, 2002.
- [4] Chazal, P., M. O'Dwyer, R.B. Reilly, "Automatic classification of heartbeats using ECG morphology and heartbeat interval features", *IEEE Transaction on Biomedical Engineering*, 51, pp.1196-1206, 2004.
- [5] Chazal, P., M. O'Dwyer, R.B. Reilly, "Automatic detection of premature atrial contraction in the electrocardiogram", *IEEE Electrotechniques and Electronics*, 9-10, 2006.
- [6] U. J. Scholz et al., "Vegetative background of sleep: Spectral analysis of the heart rate variability," *Physiol. Behavior*, vol. 62, no. 5, pp. 1037-1043, 1997.
- [7] J. Trinder et al., "Autonomic activity during human sleep as a function of time and sleep stage," *J. Sleep Res.*, vol. 10, no. 4, pp. 253-264, 2001.
- [8] L. Zapanta et al., "Heart rate chaos in obstructive sleep apnea in children," *IEEE Trans. Eng. Med. Biol.*, pp. 3889-3892, 2004.
- [9] R. B. Shouldice et al., "Detection of obstructive sleep apnea in pediatric subjects using surface lead electrocardiogram features," *Sleep*, vol. 27, pp. 784-792, 2004.
- [10] Q. Xue, Y. H. Hu, and W. J. Tompkins, "Neural-network- based adaptive matched filtering for QRS detection", *IEEE Trans. Biomed. Eng.*, 1992, 317-329.
- [11] MIT-BIH Arrhythmia Database, www.physionet.org.
- [12] Li C, Zheng C, Tai C, "Detection of ECG characteristic points using wavelet transforms", *IEEE Trans on Biomed Eng*, 1995, 42:21-28.
- [13] Moreas J., Seixas M., Vilani F., Costa E., "A QRS complex detection algorithm using electrocardiogram leads", *Comp in Card*, 2002, 29:205-208.

- [14] Englese WAH, Zeelenberg C, "A single scan algorithm for QRS detection and feature extraction", IEEE Comp in Card, 1979, 37-42.
- [15] Pan J, Tompkins W, "A real-time QRS detection algorithm", IEEE Trans Biomed Eng, 32:230-236, 1985.
- [16] Ligtenberg A, Kunt M, "A robust-digital QRS detection algorithm for arrhythmia monitoring. Computers and Biomed Res, 1983, 16:273-286.
- [17] Alvarado, C. Arregui, J. Ramos, J. Pallas-Areny, R., "Automatic detection of ECG ventricular activity waves using continuous spline wavelet transform", Proceedings of the International Conference on Electrical and Electronics Engineering (ICEEE) and XI Conference on Electrical Engineering (CIW2005) IEEE, 2005, page(s):189-192
- [18] Fei Zhang; Yong Lian., " Novel QRS Detection by CWT for ECG Sensor", Biomedical Circuits and Systems Conference, 2007. BIOCAS 2007. IEEE, 2007, page(s):211-214
- [19] V.S. Chouhan and S.S. Mehta, "Detection of QRS complexes in 12-lead ECG using adaptive quantized threshold" International Journal of Computer Science and Network Security, 2008, Vol. 8, No.1, pp. 155-163.
- [20] J.L. Willems, "Common Standards for quantitative electrocardiography", ACCO Publ, CSE multilead atlas dataset-3, CSE Project, Leuven, Belgium, 1988, pp. 1-341.
- [21] E. Braunwald, D. P. Zipes, P. Libby, R. Bonow, "Braunwald's Heart Disease: A Textbook of Cardiovascular Medicine, Single Volume" Saunders, 2004, 7th edition.
- [22] Pang, L.; Tchoudovski, I.; Braecklein, M.; Egorouchkina, K.; Kellermann, W.; Bolz, A., " Real time heart ischemia detection in the smart home care system", IEEE-EMBS, 2006, Volume , Issue , 17-18, Page(s):3703 – 3706.
- [23] Chouhan, V.S., Mehta, S.S., "Total Removal of Baseline Drift from ECG Signal", Proceedings of the International Conference on Computing: Theory and Applications (ICCTA'07), 2007, page(s): 512-515, March.
- [24] Gari D. Clifford, Francisco Azuaje, Patrick McSharry, "Advanced Methods And Tools for ECG Data Analysis," *Artech House Publishers*, 2006, 1st edition.

Authors



Mohamed Elgendi received a B.S. degree in Computer Engineering from the High Institute of Engineering, October 6 University, Egypt, in 2000, and a M.E. degree in Electrical Engineering from Charles Darwin University, Australia in 2006.

He is currently working towards a Ph.D. degree in Biomedical Engineering at Charles Darwin University. His research interests include Biomedical Signal Processing, System Identification and Data Modelling.



Mirjam Jonkman is lecturer Biomedical Engineering at Charles Darwin University. Her current research interests include Biomechanics and Signal Processing of Biomedical Signals.



Friso De Boer is currently the Head of the School of Engineering and Information Technology in Charles Darwin University, Australia. His research interests include System Identification, Signal Processing and Control.